

Applying GPR and Laser Scanner Techniques to Monitor the Ossoue Glacier (Pyrenees)

Mariano del Río¹, Ibai Rico², Enrique Serrano³ and Juan J. Tejado⁴

¹Dept. Física Aplicada, Escuela Politécnica, Universidad de Extremadura, Avda. de la Universidad s/n, 10003 Cáceres, Spain

Email: lmdelrio@unex.es

²Dept. Geografía, Prehistoria y Arqueología, Universidad del País Vasco, Paseo de la Univeridad s/n, 01006 Vitoria-Gasteiz, Spain

Email: ibai.rico@ehu.es

³Dept. Geografía, Universidad de Valladolid, Paseo Prado de la Magdalena s/n, 47011 Valladolid, Spain

Email: serrano@fyl.uva.es

⁴Dept. Rocas Ornamentales, Productos y Obras de Construcción, Instituto Tecnológico de Rocas Ornamentales y Materiales de Construcción (INTROMAC), Avda. De la Univeridad s/n, 10003 Cáceres, Spain

Email: jjtejado@intromac.com

ABSTRACT

The Ossoue glacier in the Vignemale massif (3,298 m) is currently the longest and second largest of the Pyrenees (1,400-m length, 50-ha area), and the only one presenting glacier tongue morphology. We describe 50 MHz ground penetrating radar (GPR) and laser scanner surveys from which we assess the current state and dynamics of the glacier. In 2011, nearly 1,900 m of GPR profiles over the upper half of Ossoue glacier yielded up to 45 m of depth, an average value of 30 m thickness of the subglacial layer, and internal structure and layering. We compare the results with those from a study in 2006 of the same glacier, showing similar bedrock morphology with slightly less overall ice thickness than in 2011. Laser scanner surveys at the snout showed thinning rates of 3.32 m between 2010 and 2011, 4.15 m between 2011 and 2012, and an average loss of 7.47 m between 2010 and 2012. Present-day changes in Ossoue glacier are characterized by extensive thinning caused by melting and collapse of the ice mass. If these thinning rates are maintained, Ossoue glacier will vanish within 35 yr.

Introduction

The 21 present-day glaciers of the Pyrenees are losing mass quickly. The Equilibrium Line Altitude (ELA) is close to their summits, so that they are in critical imbalance with climatic conditions (Gonzalez *et al.*, 2008). The 10 glaciers on the Spanish side and 11 on the French side cover a total of only 450 ha. Because of their small size, low altitude, and low latitude location, these glaciers are recognized as highly sensitive geo-indicators of climatic variations (Grunewald and Scheithauer, 2008; Serrano *et al.*, 2010; Serrano *et al.*, 2011). Together with the ice masses located in the Cantabrian Mountains, Maritime Alps, Italian Apennines, and the mountains of the Balkan Peninsula, the Pyrenean glaciers are categorized as part of the Southern European glaciers.

The Ossoue glacier (Fig. 1) is located on the northeast side of the Vignemale peak (3,298 m a.s.l., 42°46'16" N / 0°08'33" W) in the Vignemale massif

(Pyrenees National Park, France). The bedrock beneath the glacial sediment is marble limestone, and the general relief of the area is the result of Quaternary tectonic, glacial, and periglacial processes. Precipitation in the area ranges from 2,000 to 2,500 mm/year. The study glacier is the second largest of the Pyrenees (just after the Aneto glacier), being 1,400-m long, 400-m wide, and 50-ha in area. The morphology of this temperate glacier consists of an upper plateau, which accounts for about two-thirds of its area (René, 2007) developing into a glacier tongue (at 2,650 m a.s.l.).

Three small glaciers within the area of the Vignemale massif (Ossoue, Petit Vignemale, and Oulettes de Gaube) lay above 2,600 m a.s.l., with each located in glacial cirques of different orientations. They have followed the de-glaciation trends of the Pyrenean and other European glaciers, losing 30–100% of their volume since the end of the Little Ice Age (LIA) (Hughes *et al.*, 2006; Gonzalez *et al.*, 2008; Grunewald and Scheithauer, 2008; Steiner *et al.*, 2008). For the

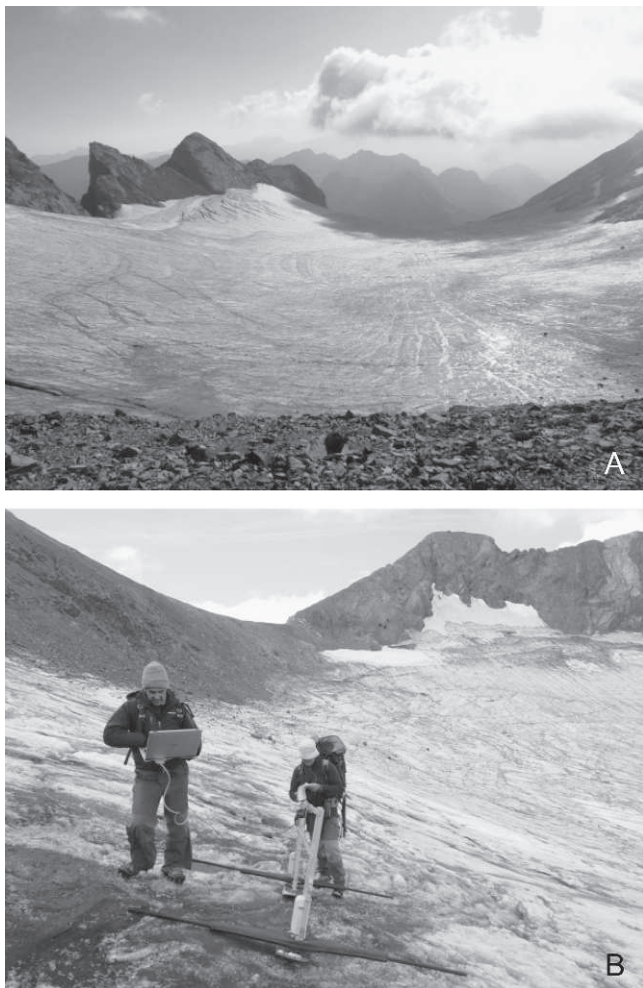


Figure 1. Glacier plateau view from west to east (A) and GPR measurements near the top, at the southern area of the glacier (B).

Ossoue glacier in particular, previous studies have allowed the evolution of its shape and areal extent from the LIA maximum in the 17th century to the last decades to be reconstructed in detail (Russell, 1908; Schrader, 1936; Martínez and Arenillas, 1988; Serrano and Martínez, 1994; Grove and Gellatly, 1995; René, 2001; René, 2011). The Ossoue glacier (like the Pyrenean glaciers) originated and developed during the LIA (González *et al.*, 2008; Martínez de Pisón and Álvaro, 2007), and therefore the remaining ice is an inheritance of this last historical glaciation (Fig. 2). In 2006, Pierre René conducted the first GPR study on the glacier, establishing a maximum depth of 50 m (René, 2007). We compare that work with the results of our study to detect glacier changes and assess the methodologies we used.

Current glacial processes in the Ossoue glacier are characterized by melting and internal motion of the ice mass. Accumulation only occurs in the northern part of

the plateau, where the west-east alignment of peaks creates a wind shadow promoting the retention of snow. This is related to the asymmetry and greater depths of the subglacial bedrock towards the north of the glacial plateau. Large transverse crevasses in this area are also evidence of the internal motion of the ice mass. However, as the conditions for glacial dynamics have worsened over the last few decades, this glacier has suffered a continual negative mass balance and disequilibrium (René, 2011). This instability is clearly reflected at the glacier front, where ice melting and collapse are the main active processes.

The present existence of the glacier is explained by topoclimatic factors such as the elevated position of the plateau (3,000 m) and the wind-blown snow effect. These topographic factors will define the response of the glacier in the short term, while climate change and general environmental conditions will determine its survival in the medium to long-term.

Our objectives were to determine the current state and dynamics of the Ossoue glacier and to compare them with previous work. We focus on the internal structure of the plateau and the surface altimetry changes at the glacier front using ground penetrating radar (GPR) and laser altimetry, respectively.

Methods

Ground penetrating radar (GPR) is now a common technique in glaciology because of its usefulness in determining ice depth and structure (Schwamborn *et al.*, 2008; Arcone and Kreutz, 2009; Del Río *et al.*, 2009; Monnier *et al.*, 2009; Shean and Marchant, 2010; Arcone *et al.*, 2013). The GPR field work of the present study was performed over two days in late August 2011 (Fig. 1). A helicopter transferred the equipment and researchers up to Coll Cervillonar (3,100 m) where a base-camp was installed. The GPR measurements were carried out satisfactorily even though the generally irregular firn on the surface, with lack of ephemeral snow, made it hard to tow the equipment. The high levels of melting were also a handicap, with profiles often re-started to avoid supraglacial streams, pools, and moulins (vertical drainage channels on the glacier surface).

The GPR used was a RAMAC system (Måla Geoscience). At the base of the antennas we placed two auxiliary wooden structures that functioned as skis. The final sampling frequency and time window were set to reach a maximum depth of 60 m, assuming an electromagnetic (EM) wave velocity in ice of 0.16 m/ns. Fifty geo-referenced radargrams were acquired with a 50 MHz (unshielded) GPR antenna, creating five profiles on the glacier — two longitudinal and three

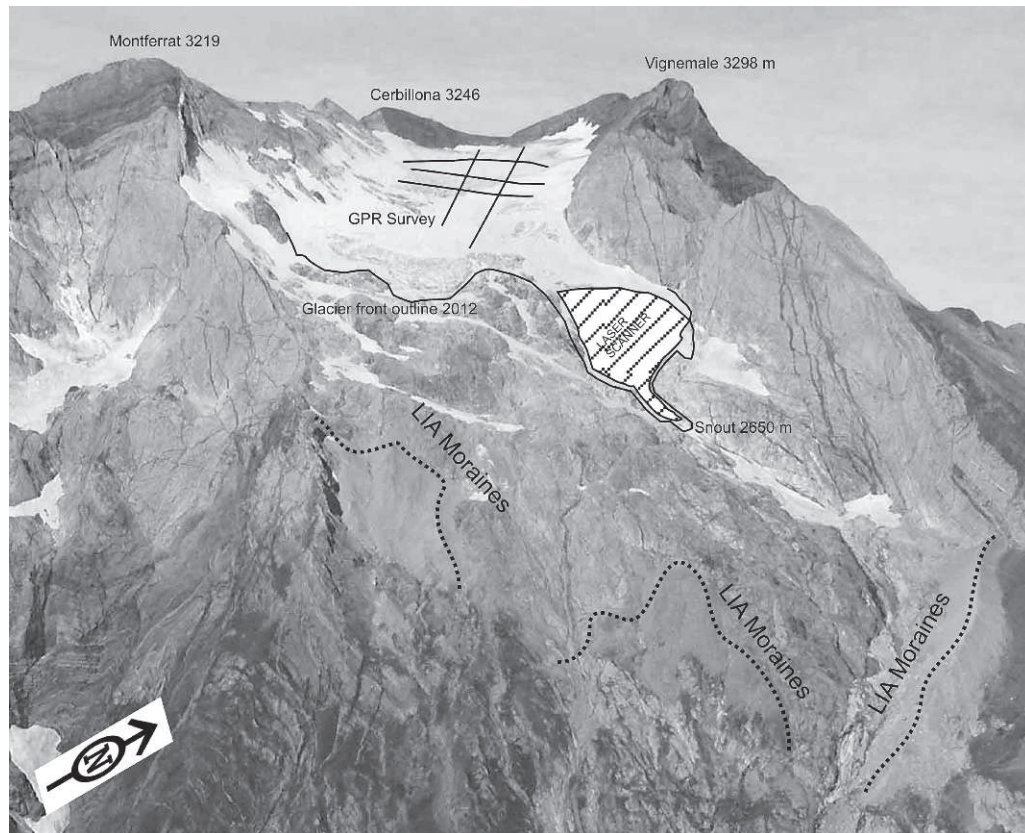


Figure 2. View of the eastern side of Vignemale massif and the glacier front of the Ossoue glacier including the LIA moraines, scanned area and GPR profiles. The picture shows the extent of ice during the LIA and the glacier retreat during the last two centuries (Source: P. René, modified by authors).

transversal (1,900 m of transects, Fig. 3). The lower section of the glacier was excluded from study because of large crevasses and water draining on the surface. We also acquired two radargrams using the common midpoint (CMP) technique with unshielded 50 MHz and 200 MHz GPR antennas to determine the radar ice velocity.

Glacier surface altimetry changes were estimated using the Terrestrial Laser Scanner (TLS) technique with 12-mm accuracy (Topcon Imaging Station) (Fig. 4). The relatively recent use of TLS on mountain glaciers is proving to be fast, practical, and relatively low-cost (Bauer *et al.*, 2003; Avian and Bauer, 2006; Kerr *et al.*, 2009; Schwalbe *et al.*, 2008; Abellán *et al.*, 2010). The Topcon Imaging Station acquired measurements at a rate of 20 p/s (points per second) for points in the range 0–120 m, and 1 p/s beyond that distance. Using a 700-nm wavelength allows high reflectivity on ice and snow. This is the first time that TLS has been applied to the Ossoue glacier.

The glacier front was scanned in the summers of 2010, 2011, and 2012. The glacier is at about three hours march (1,000 m difference in altitude) from the last motorized access point. The glacier snout was scanned

from the same position during each campaign. The number of measured locations depended on the reflectivity of the ice and the meteorological conditions, but was always between 2,000 and 2,500 points per campaign. Reflectivity of the scanned area was generally good, but in some marginal areas it was lower with the consequent appearance of “shadows.” The raw data were processed in a standard GIS program, which included data normalization (distribution) and structural analysis and kriging (rational quadratic semivariogram). In the kriging interpolation, the normalized root-mean-square deviation for all elevations was between 1.22 and 1.08 at the 98% confidence level, allowing an interpolation accuracy of 1–2 cm. The raster digital elevation models (DEMs) of different years were compared to infer the changes in surface altimetry.

Results

Internal Structure

The CMP radargram results and GPR profiles are compared with a previous GPR survey carried out in 2006 by a French team.

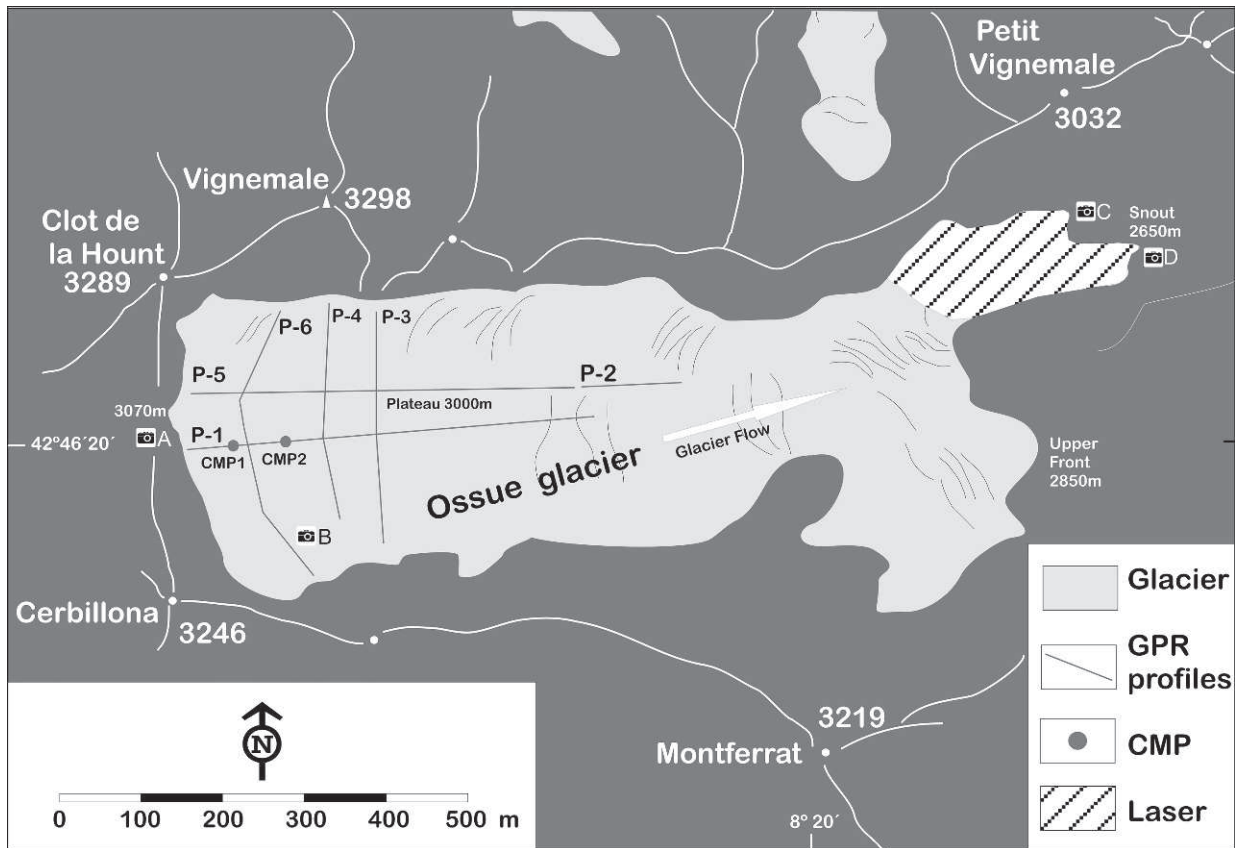


Figure 3. Location of geodetic control lines of the GPR survey and Terrestrial Laser Scanning survey. A, B, C and D indicate the points where the pictures of Figs. 1 (A, B) and 4 (C, D) were taken.

CMP radargrams. The CMP radargrams did not allow us to determine the average radar ice velocity from the glacier surface to the bedrock. We believe that this was caused by the irregularities of the terrain. Nevertheless, we obtained values for the ground wave (GW) velocity: 0.181 m/ns (CMP1 with the 50 MHz antenna) and 0.189 m/ns (CMP2 with the 200 MHz antenna). Both of these values are greater than the standard radar ice velocity (0.150–0.173 m/ns) and lower than the snow velocity (0.212–0.245 m/ns) (Brandt *et al.*, 2007), but are consistent with the value of 0.19 m/ns reported as an accumulation area (snow/firn) propagation velocity (Moorman and Michel, 1998).

GPR profiles. To facilitate the interpretation of the radargrams, we modified certain parameters. In particular, by adjusting the first arrival time, applying some post-processing routines (stacking (four traces), background removal and running average), and by increasing the image contrast, we obtained a more accurate location of the ice–ground interface. The original radargrams had many hyperbolic diffractions and reflections. The stacking of traces reduced random and variable portions of the reflected wave and aided in

identifying the bedrock topography and underlying till (Arcone *et al.*, 2013). We assumed the same EM wave propagation velocity as the previous work (0.16 m/ns; René, 2007) to obtain depth values and to compare our results with previous profiles of the same glacier (René, 2007).

The P1 profile was acquired following the central longitudinal axis of the glacier (west to east) with a length of 437 m (Fig. 3). There are various GPR sections comprising this profile (Fig. 5). First, there is a steep 50-m long section in which the ice/glacial-bedrock signal is sharp at an ice depth of 30 m. Then there is a short ascent, followed by the bedrock dropping to 45 m at a distance of 100 m from the start of the profile. Further down, interpretation becomes problematic because the signal is blurred and disturbed. A careful analysis of the signal points, however, indicate the likely presence of a thick subglacial layer formed by rocks, ice, water, and fine sediment at the interface of the ice and glacial bedrock. The presence of fractured ice down to the basal regime is a common feature of small glaciers (Lawson *et al.*, 1998). Therefore, accurate determination of the position of the actual bedrock becomes difficult. Figure 5 shows the interpreted (dotted lines) depth at

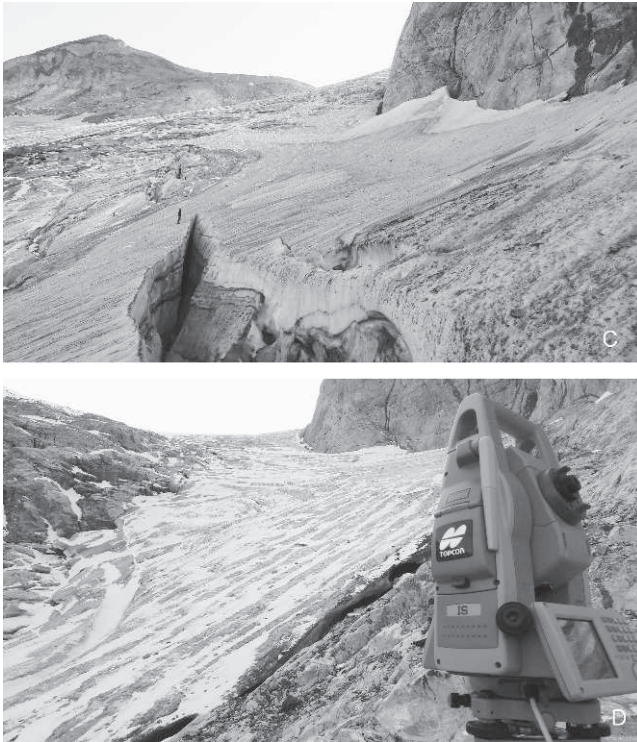


Figure 4. Glacier front area (C) and TLS measurements (D).

which the thick subglacial layer is detected. This layer appears to rise steadily up to 20 m at the end of the profile. Significant hyperbolic reflections also appear close to the surface beyond 200 m from the start, likely caused by the visible moulin network on the glacier surface (represented by circles in Fig. 5).

As stated above, the Ossoue glacier originated during the LIA, reaching its maximum extent in the 17th century and showing a major second re-advance in the mid 19th century (Grove and Gellatly, 1995; González *et al.*, 2008). Today, the associated moraines are clearly visible, separated more than 700 m from the current glacier front position (Fig. 2). Taking into account the notable size of the glacial deposits and ice depth during the LIA, about 105-m depth, we infer that the Ossoue glacier was capable of producing and releasing large amounts of till. Moreover, the presence of a weak lithology (limestones and marbles) promoted rock fracture, plucking, quarrying and grinding of the transported materials. Despite the decreased erosional capacity of the glacier since the end of the LIA, it is presumable that a layer of subglacial and englacial sediments still remains within the ice mass. This is consistent with the current presence of the subglacial till layer detected in the GPR radargrams.

The 488-m long P5 + P2 profile runs parallel to P1 (Fig. 3). Its interpretation is similar to that of P1, but

now the bedrock first descends to 35 m (70 m from the start) (Fig. 5), and, after a short ascent, it drops again to 40 m (at 130 m from the start). The same subglacial debris layer appears to slightly disturb the signal, but in this case there are no hyperbolic reflections near the surface. As these hyperbolic reflections do not appear on the surface, they can be interpreted as the response to the presence of rocky fragments embedded in the ice.

The transverse profiles, P6, P4, and P3, are parallel to each other and ordered from the highest part of the glacial plateau downwards (Fig. 3). P6 (396-m long) exhibits an abrupt descent from the start of the profile to 110 m south (35-m deep) (Fig. 6). The ice-rock interface then rises steadily to the surface. This pattern is repeated in the other two profiles; P4 (236 m) reaches its deepest point of 40 m at a distance of 70 m from the start of the profile, and P3 (301 m) reaches its deepest point of 30 m at a similar distance.

The GPR measurements thus allow us to summarize the ice depth and the morphology of the subglacial bedrock at the plateau of the Ossoue glacier. The maximum ice depth is 45 m at the higher part of the plateau, approximately at the location of CMP2 ($0^{\circ} 08' 876''$ W, $42^{\circ} 46' 257''$ N). The morphology of the subglacial bedrock seems to be characterized (from west to east) by a 45-m deep rock basin, followed by an ascendant rock bar, and then a large area of debris glacial materials with an average depth of 30 m. Transversally, the radargrams show deeper and steeper values close to the mountain peaks surrounding the plateau to the north. The quality of the bottom signal in the radargrams changes significantly from west to east, with notably better resolution in the upper part of the glacier and a distorted signal in lower sections caused by greater water drainage and the accumulation of sediments and rocks from the upper areas.

Comparison with previous GPR measurements. In 2006, the Association Moraine carried out a GPR study at the same site (René, 2007). They used a pulse EKKO 100 GPR system with a 50 MHz antenna, recorded seven profiles on the plateau, and measured a maximum depth of 50 m. The positions of our profiles correspond approximately to four of theirs. Both data sets show a generally coherent picture of the ice depth and subglacial morphology: from west to east, a steep overdeepened basin with clear GPR signal, followed by another basin characterized by a disturbed signal and the presence of meltwater and moulins (René, 2007). Signal disturbance begins approximately at the same point, about 100–150 m from the start of the longitudinal profiles. Transversally, the 2006 radargrams also show a clear asymmetry with more abrupt bedrock below the Vignemale summit and the adjacent peaks.

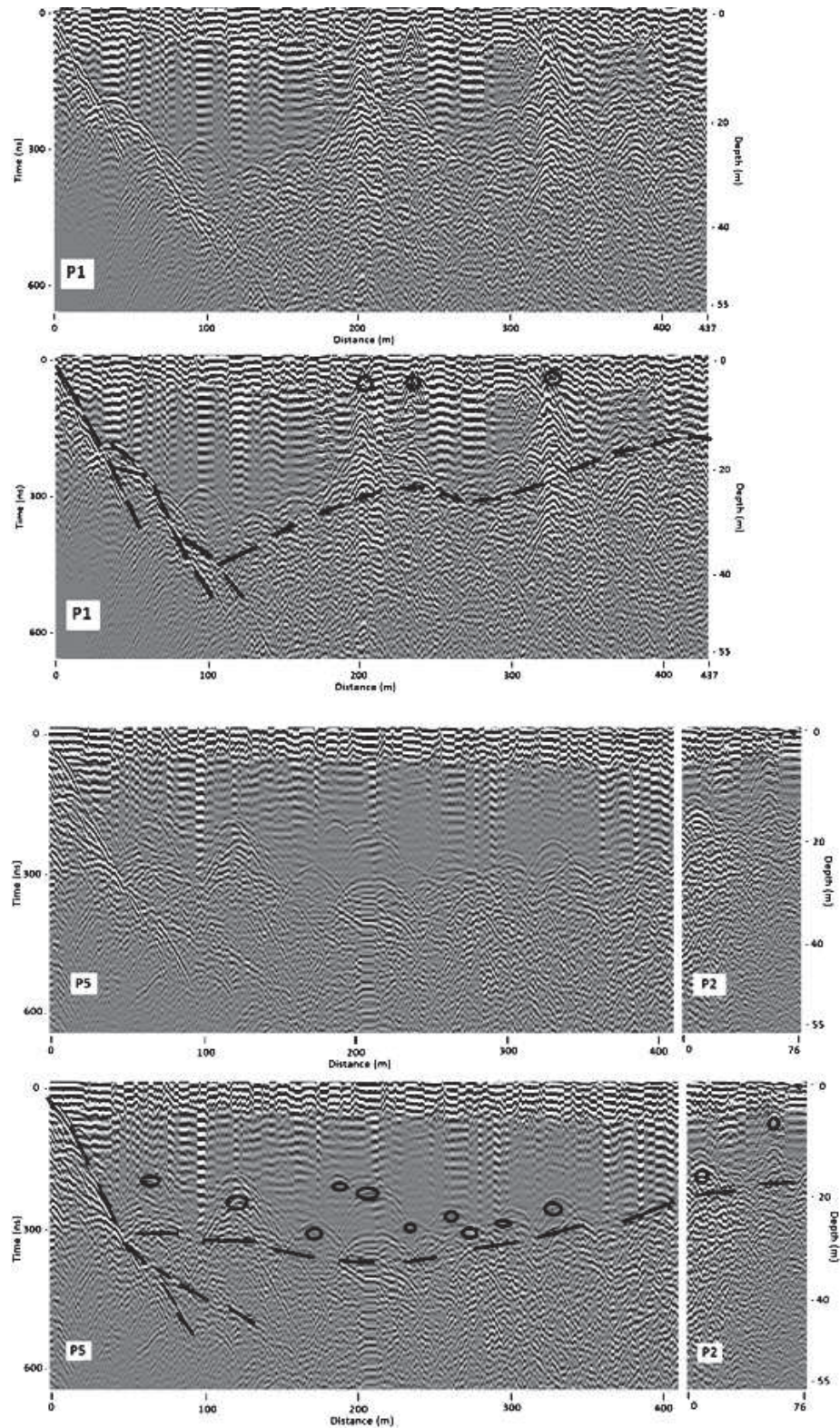


Figure 5. Processed and interpreted longitudinal (P1, P5 + P2) profiles obtained with the 50 MHz antenna. On the left is the time scale and on the right the depth scale, assuming 0.16 m/ns ice velocity.

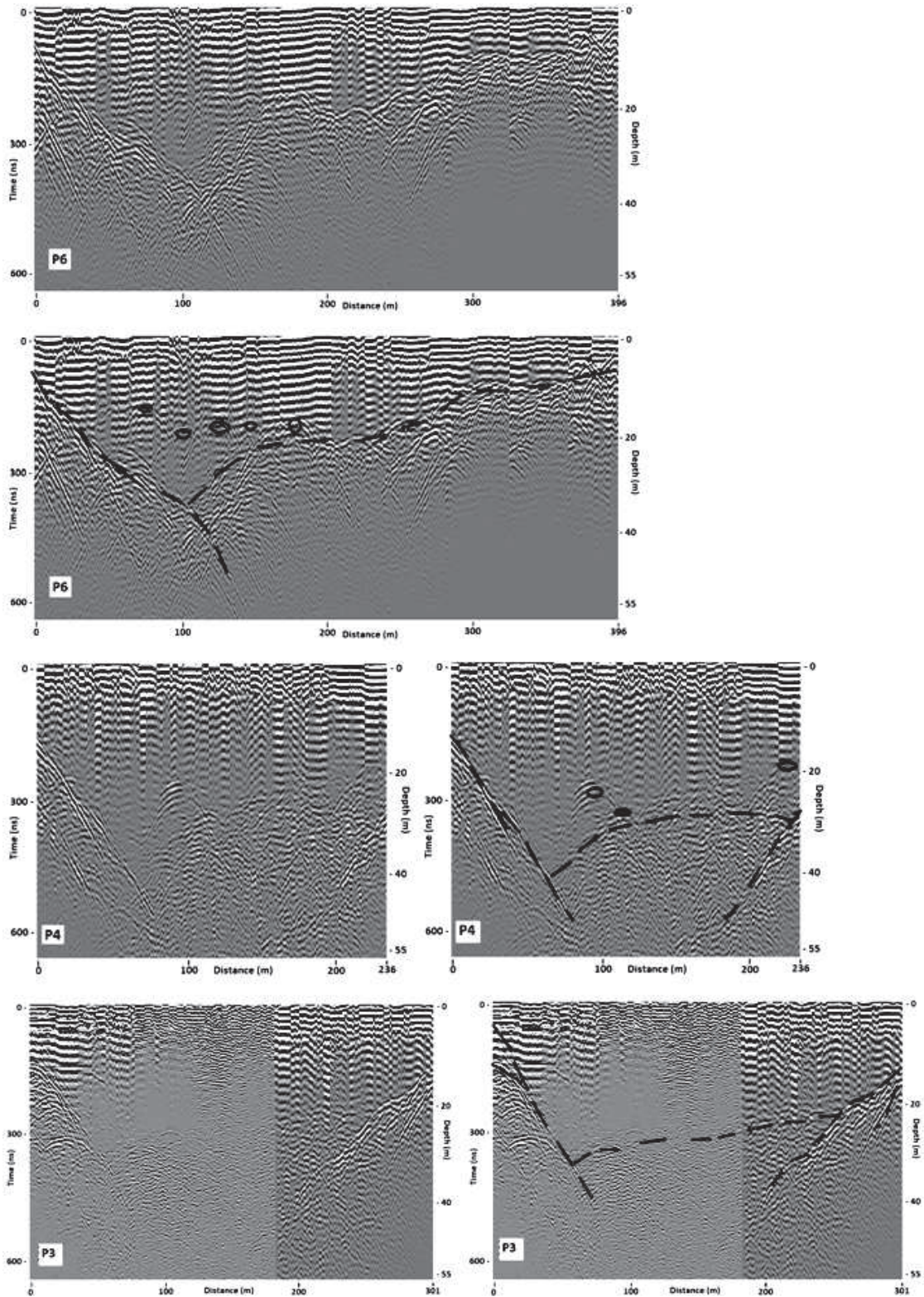


Figure 6. Processed and interpreted transversal (P6, P4, P3) profiles obtained with the 50 MHz antenna. On the left is the time scale and on the right the depth scale, assuming 0.16 m/ns ice velocity.

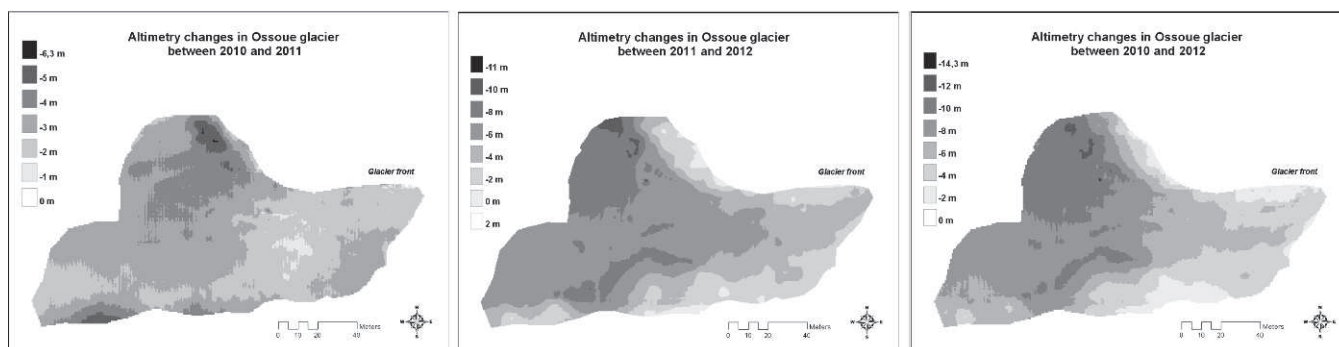


Figure 7. Glacier surface altimetry changes at the front of the Ossoue glacier for the 2010–2012 period.

The ice depths obtained in the present study, while similar, are therefore slightly less than the 2006 measurements. Nevertheless, a definitive assessment of any depth changes that may have occurred is difficult given that the resolution of the 50 MHz antennas used in the two studies is about 1.6 m (one half wavelength).

Surface Altimetry

A comparison of the scanned surfaces in subsequent years provides insight into the glacier's surface altimetry dynamics. A comparison of the 2010 and 2011 surfaces is shown in Fig. 7 as glacier altimetry change maps. They show that the glacier's snout is mainly characterized by ice thinning between 2010 and 2011. Maximum ice-loss values reach 5–6 m in some areas of the snout (north margin), linked to processes of collapse. Overall, the values range from 3 to 4 m of ice loss, the average ice thinning being 3.32 m for the 2010–2011 period. The the current front seems to be losing less ice than the upper (western) section. Comparing the scanned surfaces of 2011 and 2012, one infers an average ice loss of 4.15 m. Ice thinning has intensified in the upper western section, with extensive areas showing a decrease in thickness of 4–7 m. The glacier front presents greater instability with moderate thinning.

Overall, glacier dynamics between 2010 and 2012 may be characterized by an extensive and dramatic loss of ice. The average value determined for the scanned surface is 7.47 m of ice thinning during this two-year period. The greatest thinning is found in the upper part of the scanned area (~14 m), while the front presents a steadier situation. This process can be explained by the concave relief of the very front of the glacier, acting like a snow retention area (windblown spindrift effect). On the other hand, the upper western front is steeper and thus less prone to snow accumulation. Overall, glacier thinning governs the snout of the glacier except in the concave section of the front where reduced accumulation occurs because of local topoclimatical effects. In summary, the present-day changes at the front of the

Ossoue glacier are characterized by extensive ice thinning caused by the melting and collapse of the ice body.

We use the Johannesson (Johannesson *et al.*, 1989) volume response time formulae, later improved (Raper and Braithwaite, 2009), to estimate the lifetime of the glacier in the near-future: $t = (H / -b) \times 2.9$ where t is response time, H is maximum thickness of ice, $-b$ is ablation per year at the terminus and 2.9 is the applied constant to include topography, altitude range and vertical mass balance factors (Raper and Braithwaite, 2009). The GPR results show a maximum ice thickness of 45 m depth, and the TLS data show an ablation of -3.7 m per year at the terminus. The result is that, if the current trend continues, the lifetime of the Ossoue glacier will be 35 yr, vanishing around 2047. This result is consistent with the estimations inferred from the ELA changes (González-Trueba *et al.*, 2008), which indicate that glaciers of the Pyrenees will disappear by 2050. Therefore, glacial activity in the Ossoue glacier is bound to cease between 2045 and 2055.

Conclusions

The GPR survey carried out in the 2011 summer, total length 1,900 m, has contributed to a better understanding of the basal topography, surface altimetry changes, internal structure and characteristics of Ossoue glacier. The radargrams indicate that the subglacial bedrock possibly consists of two overdeepened rock basins, separated by a rock bar. The maximum ice depth was determined to be 45 m in the upper overdeepened rock basin ($0^{\circ} 08' 876''$ W, $42^{\circ} 46' 257''$ N).

Despite the difficulty presented by the distortion of the ice depth values caused by moulins, drainage water, and subglacial materials, it was possible to identify a thick subglacial layer having an average depth of 30 m. The ice depth on the plateau appears to be greater towards the north, close to the maximum

altitudes near the Vignemale peak. Our approach allowed us to measure almost 2,000 m of profiles in two days of work.

The comparison with the 2006 survey (René, 2007) showed the results to be similar regarding bedrock morphology. However, the overall ice thickness was slightly less in 2011. Methodologically, the two studies match in the high quality of the signal in the upper part and distortions in the lower sections. This coherence between the two studies confirms the reliability of using GPR with regard to mapping bedrock morphology and ice depth.

The laser scanner measurements indicate that present-day changes at the front of the Ossoue glacier are characterized by extensive ice thinning caused by the melting and collapse of the ice body. The average ice loss during the 2010–2012 period was -7.47 m; -3.32 m (2010–2011) and -4.15 m (2011–2012). If this rate is maintained, the glacier will disappear within the next 35 years. Future measurements will allow a better understanding of the state and dynamics of this glacier in the context of global change and the Pyrenean high mountain environment.

Acknowledgments

This research has been partially funded by project CGL-2010-19729, Spanish Government. We would like to thank Pierre René for his collaboration and Idoia Urrutia for the help provided with GIS. We are also grateful to the Pyrenees National Park authorities, in particular to Eric Sourp and also to José Luis Sánchez, Javier de Blas and Martín Merino for technical support with the GPR and TLS equipment.

References

- Abellán, A., Calvet, J., Vilaplana, J.M., and Blanchard, J., 2010, Detection and spatial prediction of rockfalls by means of terrestrial laser scanner monitoring: *Geomorphology*, **119**, 162–171.
- Arcone, S.A., and Kreutz, K., 2009, GPR reflection profiles of Clark and Commonwealth Glaciers, Dry Valleys, Antarctica: *Annals of Glaciology*, **50**(51) 121–129.
- Arcone, S.A., Mercer, J., and Hamilton, G., 2013, Englacial and basal void detection using helicopter-borne 200 MHz antennas: Ablation zone, Koge Bay, East Greenland: *in* Proceedings: Cryosphere Geophysics: Understanding a changing climate with subsurface imaging, Boise State Univ., Boise, Idaho.
- Avian, M., and Bauer, A., 2006, First results on monitoring glacier dynamics with the aid of terrestrial laser scanning on Pasterze Glacier (Hohe Tauern, Austria): *in* Proceedings, 8th International Symposium on High Mountain Remote Sensing Cartography, La Paz, **41**, 27–36.
- Bauer, A., Paar, G., and Kaufmann, V., 2003, Terrestrial laser scanning for rock glacier monitoring: *in* Permafrost, Phillips, M., Springman, S.M., and Arenson, L.U. (eds.), Swets & Zeitlinger, Lisse, 55–60.
- Brandt, O., Langley, K., Kohler, J., and Hamran, S.E., 2007, Detection of buried ice and sediment layers in permafrost using multi-frequency ground penetrating radar: A case examination on Svalbard: *Remote Sensing of Environment*, **111**, 212–227.
- Del Río, L.M., Tejado, J.J., De Sanjosé, J.J., Atkinson, A., Serrano, E., González, J.J., and Fernandez, A., 2009, Ice match structure and depth using GPR techniques: A first approach to the Jou Negro ice patch (Picos de Europa, Spain): *in* Proceedings: 5th Internacional Workshop on Advanced Ground Penetrating Radar IWAGPR'09, 278–284.
- González-Trueba, J.J., Martín, R., Martínez de Pisón, E., and Serrano, E., 2008, Little Ice Age glaciation and current glaciers in the Iberian Peninsula, The Holocene, **18**(4) 551–568.
- Grove, J.M., and Gellatly, A.F., 1995, Little Ice Age fluctuations in the Pyrenees: *Zeitschrift für Gletscherkunde und Glacialgeologie*, **31**, 199–206.
- Grunewald, K., and Scheithauer, J., 2008, Europe's southernmost glaciers: Response and adaptation to climate change: *Journal of Glaciology*, **56**(195) 129–142.
- Hughes, P.D., Woodward, J.C., and Gibbard, P.L., 2006, Quaternary glacial history of the Mediterranean mountains: *Progress in Physical Geography*, **30**(3) 334–364.
- Johannesson, T., Raymond, C.F., and Waddington, E.D., 1989, A simple method for determining the response time of glaciers: *in* Glacier Fluctuations and Climate Change, Oerlemans, J. (ed.), Kluwer, Dordrecht, 407–417.
- Kerr, T., Owens, I., Rack, W., and Gardner, R., 2009, Using ground-based laser scanning to monitor surface change on the Rolleston Glacier, New Zealand: *Journal of Hydrology (NZ)*, **48**(2) 59–72.
- Lawson, D.E., Strasser, J.C., Evenson, E.B., Alley, R.B., Larson, G.J., and Arcone, S.A., 1998, Glaciohydraulic supercooling: A freeze-on mechanism to create stratified, debris-rich basal ice: I. Field evidence: *Journal of Glaciology*, **44**(148) 547–562.
- Martínez de Pisón, E., and Arenillas, M., 1988, Los glaciares actuales del Pirineo español: *in* La nieve en el Pirineo Español, Ministerio de Obras Públicas y Urbanismo, MOPU, Madrid, 29–98.
- Martínez de Pisón, E., and Álvaro, S., 2007, El libro de los Hielos, Ediciones Desnivel, Madrid, 311.
- Monnier, S., Camerlynck, C., and Rejiba, F., 2009, Ground penetrating radar surveys on rock glaciers in the Vanoise Massif (Northern French Alps): *Géomorphologie*, **2**, 129–140.
- Moorman, B.J., and Michel, F.A., 1998, The application of ground-penetrating radar to the study of glacial hydrology: *in* Proceedings: Seventh International Conference on Ground-Penetrating Radar GPR '98, 27–30.
- Raper, S.C.B., and Braithwaite, R.J., 2009, Glacier volume response time and its links to climate and topography based on a conceptual model of glacier hypsometry: *The Cryosphere*, **3**, 183–194.

- René, P., 2001, Actualisation des observations sur les glaciers des Pyrénées Centrales Françaises: Journal du Parc National des Pyrenees, **10**, 9–10.
- René, P., 2007, Prospection radar au glacier d'Ossoue (Vignemale-Pyrénées) : Détermination de l'épaisseur du glacier et de la topographie du lit rocheux : Association Pyrénéenne de Glaciologie, **24**, Luchon.
- René, P., 2011, Les glaciers des Pyrénées françaises: Rapport d'étude 2010–11 : Association Pyrénéenne de Glaciologie, **27**, Luchon.
- Russell, H., 1908, Souvenirs d'un Montagnard, Imprimerie Vignancour, Pau.
- Schrader, F., 1936, Sur l'étendue des glaciers des Pyrenees 1894: *in* Pyrenees, P. (ed.), Toulouse, 201–221.
- Schwalbe, E., Maas, H.G., Dietrich, R., and Ewert, H., 2008, Glacier velocity determination from multi temporal terrestrial long range laser scanner point clouds: The International Archives of the Photogrammetry, Remote Sensing and Spatial Information Sciences: *in* XXIst ISPRS Congress, Jun, C., Jie, J., and Maas, H.-G. (eds.), **37** (B5), Beijing.
- Schwaborn, G., Heinzl, J., and Schirmeister, L., 2008, Internal characteristics of ice-marginal sediments deduced from georadar profiling and sediment properties (Brøgger Peninsula, Svalbard): *Geomorphology*, **95**, 74–83.
- Serrano, E., and Martínez de Pisón, E., 1994, Geomorfología y evolución glaciaria en el Pirineo aragonés oriental: *in* El glaciario surpirenaico: Nuevas aportaciones, Martí, C.E., and Garcia, J.M. (eds.), Geoforma Ediciones, 33–64.
- Serrano, E., Sanjosé, J.J., and González-Trueba, J.J., 2010, Rock glacier dynamics in marginal periglacial environment: *Earth Surface Processes and Landforms*, **35**, 1302–1314.
- Serrano, E., González-Trueba, J.J., Sanjosé, J.J., and Del Río, L.M., 2011, Ice patch origin, evolution and dynamics in a temperate maritime high mountain: The Jou Negro, Picos de Europa (NW Spain), *Geografiska Annaler*, **93**, 97–70.
- Shean, D.E., and Marchant, D.R., 2010, Seismic and GPR surveys of Mullins Glacier, McMurdo Dry Valleys, Antarctica: Ice thickness, internal structure and implications for surface ridge formation: *Journal of Glaciology*, **56**, 48–64.
- Steiner, D., Pauling, A., Nussbaumer, S.U., Nesje, A., Luterbacher, J., Wanner, H., and Zumbühl, H.J., 2008, Sensitivity of European glaciers to precipitation and temperature – Two case studies: *Climatic Change*, **90**, 413–441.